Critical slowing down and elastic anomaly of uniaxial ferroelectric $Ca_{0.28}Ba_{0.72}Nb_2O_6$ crystals with tungsten bronze structure

K. Suzuki,[1] K. Matsumoto,[1] J. Dec,[2] T. Łukasiewicz,[3] W. Kleemann,[4] and S. Kojima[1,*]

[1]*Division of Materials Science, University of Tsukuba, Tsukuba, Ibaraki 305-8573, Japan*

[2]*Institute of Materials Science, University of Silesia, PL-40-007 Katowice, Poland*

[3]*Institute of Electronic Materials Technology, PL 01-919 Warsaw, Poland*

[4]*Angewandte Physik, Universität Duisburg-Essen, D-47048 Duisburg, Germany*

(Received 14 February 2014; revised manuscript received 8 August 2014; published 26 August 2014)

The ferroelectric phase transition of uniaxial $Ca_{0.28}Ba_{0.72}Nb_2O_6$ single crystals with a moderate effective charge disorder was investigated by Brillouin scattering to clarify the dynamic properties. In the tetragonal paraelectric phase a remarkable softening of the sound velocity of the longitudinal acoustic mode and a significant increase in the sound attenuation were observed close to the Curie temperature $T_C = 527$ K. The intermediate temperature $T^* \sim 640$ K and the Burns temperature $T_B \sim 790$ K were determined from the temperature variation in the sound attenuation. The intense broad central peak (CP) caused by polarization and strain fluctuations due to polar nanoregions was clearly observed in the vicinity of T_C. The relaxation time determined by the CP width clearly shows critical slowing down towards T_C, reflecting a weakly first-order phase transition under weak random fields.

DOI: 10.1103/PhysRevB.90.064110 PACS number(s): 62.20.−x, 63.20.−e, 77.80.Jk, 78.35.+c

The frustration of competing interactions and a disordered structure play a dominant role in spin and dipole glasses with ferroic and antiferroic interactions, structural glasses with bond and density order parameters, and relaxor ferroelectrics (RFEs). Such disordered nonequilibrium systems show typical peculiar phenomena, such as Vogel-Fulcher freezing, nonlinear response, aging, rejuvenation, etc. Typical RFEs have disordered three-dimensional structures, such as the perovskites $Pb(Mg_{1/3}Nb_{2/3})O_3$ and $Pb(Sc_{1/2}Ta_{1/2})O_3$ or the uniaxial tetragonal tungsten bronze (TTB) $Sr_xBa_{1-x}Nb_2O_6$ (SBN) [1,2]. In these RFEs quenched random electric fields originating from charged compositional fluctuations induce the critical slowing down and the freezing into nanometric polar domains below the dielectric maximum temperature T_m. For industrial demands, lead-free RFEs, such as SBN, have recently attracted much attention because of their outstanding functional properties under emerging environmental regulations. The ferroelectric phase transitions of the SBN family have been discussed within the random-field Ising model [3,4]. SBN shows excellent dielectric [5,6], piezoelectric [7], pyroelectric [8], and photorefractive properties [9–12]. The high values of the spontaneous polarization and the electro-optic coefficient of SBN, especially for Sr-rich alloys, are affected by the smaller lattice parameters in comparison to other TTB ferroelectrics [13]. Upon heating from room temperature, SBN undergoes a ferroelectric phase transition from $4mm$ to $4/mmm$ [5]. Upon increasing the Sr content, the Curie temperature T_C decreases, and the diffusive nature increases with the increase in the random field strength, which plays a dominant role in the relaxor nature. The RFE behavior is caused by the random fields due to the charge distribution with A (i.e., A1 and A2) site disorder. In the TTB structure, 5/6 of the A (A1 + A2) sites are occupied with divalent cations, whereas the remaining 1/6 are vacancies. The relaxor nature was discussed based on the statistical models of the vacancies at the A sites [14,15].

Calcium barium niobate, $Ca_xBa_{1-x}Nb_2O_6$ (CBN), compounds also have TTB structures, and their physical properties are very similar to those of SBN, whereas their Curie temperatures T_C exceed those of SBN [16–19]. Due to the smaller ionic radius of Ca^{2+} compared to that of Sr^{2+}, most of the Ca ions occupy A1 sites, whereas most of the Ba ions occupy A2 sites. Hence, the diffusive nature is less pronounced than for SBN. Actually, the dielectric constant of $Ca_{0.28}Ba_{0.72}Nb_2O_6$ (CBN28) shows a sharp peak near T_C [20].

This fact also affects the average domain size, and domains larger than that of SBN were observed in CBN [18]. Other consequences of the weaker diffusive nature are the decrease in the index of the extended Curie-Weiss law to 1.65 and the lack of a frequency-dependent high-T shift in the susceptibility peak T_m [21]. It was assumed that the outstanding characteristics of SBN are associated with the relatively small lattice parameters [13], whereas CBN actually has lattice parameters smaller than those of SBN. Generally, in REFs, polar nanoregions (PNRs) are formed below the Burns temperature T_B upon cooling. The interaction between the acoustic phonon and the polarization fluctuations in the PNRs causes the deviation in the sound velocity at T_B from the linear dependence at high temperatures [22–24]. Upon further cooling, a dynamic to static transition of the PNRs occurs, and the growth rate of the PNRs suddenly increases at the intermediate temperature T^*, which was detected by the acoustic emission in many of the relaxors, for example, in SBN75, where $T_C = 332$, $T^* = 456$, and $T_B = 623$ K [25]. Relaxorlike behavior was also reported in $BaTiO_3$, where $T_C = 400$, $T^* = 506$, and $T_B = 530$–570 K [26]. Even though its cluster dynamics becomes much faster, relaxorlike features were observed in the paraelectric phase of $BaTiO_3$. At the Curie temperature T_C, the volume of the PNRs reaches the percolation limit where all PNRs are frozen into a stable ferroelectric domain state [27].

*kojima@ims.tsukuba.ac.jp

Recently, the relaxor nature of CBN28 was studied in the paraelectric phase by resonant ultrasonic spectroscopy (RUS) [28]. Many elastic constants were successfully determined in the paraelectric phase. Contrastingly, RUS is difficult to measure when the acoustic attenuation becomes high as in the ferroelectric phase. Here the dissipation effects are so strong that the modes of group 1 (A_g and B_{1u} symmetries), which show a significant softening near the Curie temperature, were no longer observed. In contrast, in Brillouin scattering it is possible to measure the modes even if the dissipation effects are strong, and the relaxation process can be discussed by observation of a central peak [29–31]. Whereas Brillouin scattering of SBN has been extensively studied, that of CBN has not yet been studied.

In the present study, the elastic properties and relaxation dynamics of CBN28 crystals were investigated by narrow and broadband Brillouin scattering, respectively. CBN28 crystals were grown by the Czochralski method [32]. Single crystals were cut into plates with a size of $5\times5\,\mathrm{mm}^2$ and thickness of 1 mm along the [100] and [001] directions (a and c plates, respectively) with the two surfaces being polished to optical quality. Brillouin scattering was measured in backward-scattering geometry using a tandem Fabry-Pérot interferometer and a single frequency green yttrium aluminum garnet laser at a wavelength of 532 nm [33]. The elastic properties were studied in the temperature range from room temperature to 1023 K with a free spectral range (FSR) of 75 GHz. The broad central peak (CP) appearing around T_C was also measured with a large FSR of 300 GHz to clarify the relaxation behavior of the polarization fluctuations. The heating process was first measured upon heating to 723 K, and then the cooling process was measured in order to investigate the thermal hysteresis. The high-temperature behavior was also measured up to 1023 K in order to observe the change in the elastic properties near T_B.

In the Brillouin spectra observed on the a plate, longitudinal acoustic (LA) and transverse acoustic modesand a strong elastic Rayleigh peak were observed, whereas in the spectrum of the c plate, only the LA mode was observed as shown in Fig. 1. The measured Brillouin peaks were fitted by the Voigt function, a convolution of Lorentzian and Gaussian functions, to determine the Brillouin shift (ν_B), the full width at half maximum [(FWHM) Γ_B], and the peak intensity. We then calculated the sound velocity V and amplitude attenuation α from ν_B and the FWHM of the LA peak using the equations $V = \lambda\nu_B/2n$ and $\alpha = \pi\Gamma_B/V$, where λ and n represent the laser wavelength (532 nm) and the refractive index of the ordinary or extraordinary ray, respectively. We obtained the values of the ordinary n_o and extraordinary refractive indices n_e for the incident laser wavelength of 532 nm with fitting using a fourth-order function on the values in Ref. [34]. In the calculation of the sound velocity and attenuation, the value of n_e was used for the scattering geometry $a(cc)\bar{a}$ by the Porto notation, whereas the value of n_o was used for the scattering geometries $a(bb)\bar{a}$, $c(aa)\bar{c}$, and $c(bb)\bar{c}$.

The observed temperature dependences of the LA sound velocity along the c axis and sound attenuation α are shown in Fig. 2. We determined $T_C = 527$ K from the minimum temperature of the sound velocity upon heating. The velocity shows a remarkable softening towards T_C caused by the interaction between the PNRs and the LA mode above the T_C. This behavior above T_C is in agreement with the RUS result [35] within experimental uncertainty. In addition, upon further heating, its intensity increases by the increase in the photoelastic constant. At the same time, the temperature

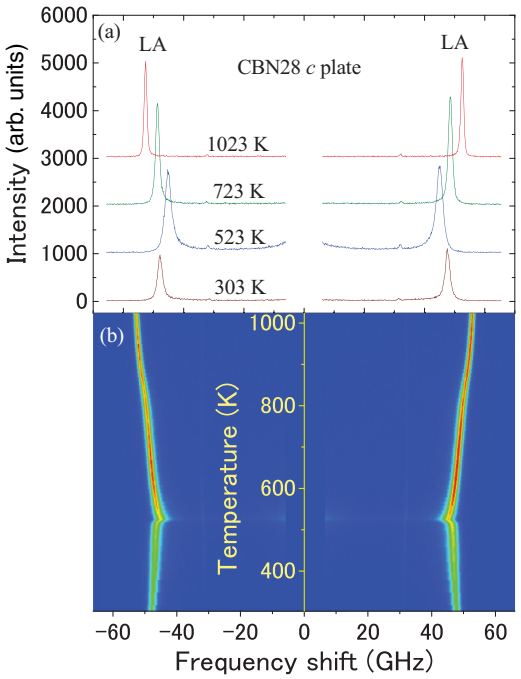

FIG. 1. (Color online) (a) Temperature dependence of the Brillouin spectra of CBN28 (c plate) (FSR = 75 GHz, scan range = 66.5 GHz). (b) Contour map of the narrow-band scattering intensity of CBN28 (c plate) vs temperature. The elastic scattering was removed in the vicinity of 0 GHz.

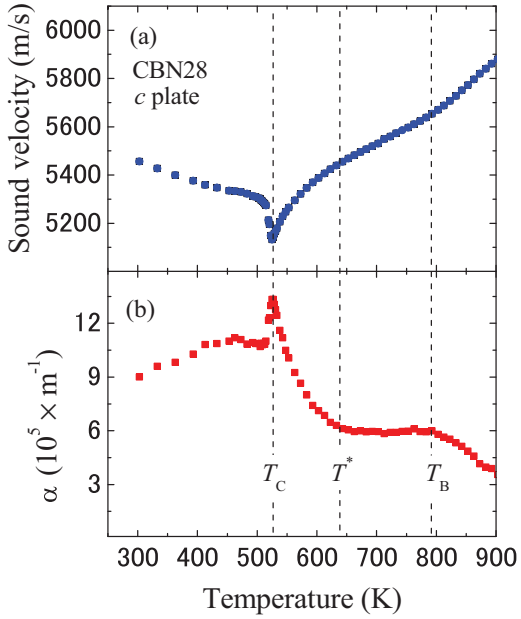

FIG. 2. (Color online) Temperature dependences of (a) the sound velocity V and (b) sound attenuation coefficient α of a CBN28 single crystal (c plate).

dependence of the sound attenuation α shows a sharp peak at T_C. Such a divergent phenomenon of the sound attenuation reflects the dissipation of the LA mode by the interaction with dynamic PNRs [36]. Below T_C, the heating and cooling processes show a noticeable difference, which is due to the metastable irreversible domain structure caused by the finite cooling rate [37,38]. As shown in Fig. 2 the sound attenuation shows the deviation from the linear change below $T \sim 640$ K as was reported also in SBN61 [30]. A deviation from the linear change is also observed near $T \sim 790$ K. These anomalies can be attributed to the characteristic temperatures of the PNRs, i.e., $T^* \sim 640$ and $T_B \sim 790$ K. Whereas in SBN75, $T_B - T_C = 309$ and $T^* - T_C = 124$ K [25], we obtain similar, albeit slightly lower values in CBN28, $T_B - T_C = 263$ and $T^* - T_C = 113$ K. Obviously, SBN75 and CBN28 behave similarly in the precursor temperature region thus defining a common characteristic of the charge-disordered TTB structure.

Our values of T^* and T_B are significantly lower than those reported by Pandey *et al.* [28,35], $T^* \sim 800$ and $T_B \sim 1100$ K. This discrepancy probably arises from the different qualities of the investigated CBN samples. Although our samples were colorless, those investigated in Refs. [28,35] were "*nearly colorless*" or even "*light yellow*," a possible indication of an oxygen deficiency as observed in numerous oxides and generally explained by deep electron traps [39]. Such a defect structure may be related to the very high temperature found in the experiments of Pandey *et al.* [35]. Very likely, CBN tends to become chemically unstable in a way similar to that reported for the homologous TTB compound SBN [34]. That is why we believe that our results are more appropriate for the pure CBN samples being colorless both before and after the experiments.

The spectra of the *a* plate show a notable temperature dependence, and the broad CP appears around T_C as shown in Fig. 3. This CP is the characteristic of the polarization fluctuations along the ferroelectric *c* axis as was extensively observed for RFEs [29,36,37]. Between $T_B \sim 790$ and $T_C \sim 527$ K, the polarization fluctuations of the PNRs along the ferroelectric *c* axis were observed as the CP, which is common in Refs. [36–38]. The remarkable temperature dependence of the CP upon cooling was observed as shown in Fig. 3. The CP intensity I_{CP}, related to the relaxation strength increases from a high temperature down to T_C as shown reciprocally by T/I_{CP} in Fig. 4. The FWHM of the CP Γ_{CP} shows a minimum at T_C. The intensity I_{CP} is related to the static susceptibility $\chi(0)$ by the equation $I_{CP} = I_0 k_B T \chi(0)$, where k_B is the Boltzmann constant and I_0 is a constant depending on the experimental condition of the scattering geometry. The relaxation time was calculated using the equation $\tau = 1/\pi\Gamma_{CP}$. The temperature dependences of the inverse of $\chi(0)$ and τ are shown in Fig. 4. The critical behavior of τ in the vicinity of $T_C = 527$ K is given by

$$\frac{1}{\tau} = \frac{1}{\tau_0} + \frac{1}{\tau_1}\frac{(T - T_C)}{T_C} \quad \text{for} \quad T > T_C, \tag{1}$$

with the best-fitted parameters $1/\tau_0 = 6.76\times10^{11}$ and $1/\tau_1 = 1.77\times10^{12}\text{s}^{-1}$. The inverse relaxation time τ^{-1} indicates the critical slowing down of the polarization fluctuations along the ferroelectric *c* axis as similarly observed at the ferroelectric phase transition of PSN-30PT [36]. In contrast, the relaxation times of SBN61 and SBN75 did not show any clear critical

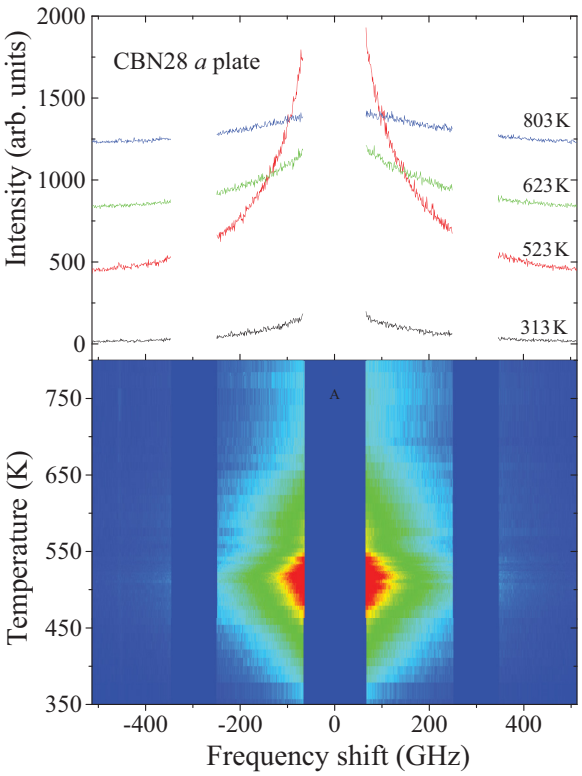

FIG. 3. (Color online) (a) Temperature dependence of the broadband scattering intensity from a CBN28 single crystal (*a* plate) (FSR = 300 GHz, scan range = 518 GHz). (b) Contour map of the broadband scattering intensity from a CBN28 single crystal (*a* plate) vs temperature. The elastic scattering was removed in the vicinity of 0 and ± 300 GHz.

slowing down due to the strong diffuseness of their phase transitions [29,31]. Their relaxation times gradually change and are shorter than the relaxation time of CBN28. The difference in the relaxation times can be attributed to the different sizes of the PNRs. These may be discussed on the basis of the site occupancy. In a previous study, it has been shown that CBN28 and SBN61 have a similar unit-cell size [13,28]. On the other hand, the Ca^{2+} ion radius is

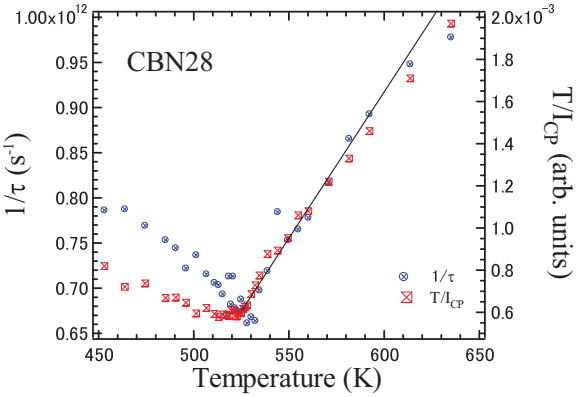

FIG. 4. (Color online) Temperature dependences of the inverse relaxation time determined from the CP width and the temperature divided by the CP intensity in a CBN28 single crystal (*a* plate).

approximately 7% smaller than that of Sr^{2+} and approximately 17% smaller than the Ba^{2+} ion in the 12-fold coordination of the A1 site. Hence, Ca^{2+} prefers the smaller A1 sites rather than the bigger A2 ones as compared to the Sr^{2+} ions. Actually, Sr^{2+} occupies 71.84% of the A1 sites and 40.38% of the A2 sites, whereas the Ca^{2+} ions occupy only the A1 sites [21]. Thus the lower disorder of the Ca^{2+} and Ba^{2+} ions is the origin of the weak random fields in CBN28, which prefers a longer-range order and causes the weakly first-order phase transition of the order-disorder type with a sharp critical slowing down in the vicinity of T_C. In addition, the size of the domains is greater in CBN28 [18], therefore, the PNRs, which grow into polar domains upon cooling, can also be larger. Since the bigger PNRs slowly fluctuate, the relaxation time of CBN28 is longer than that of SBN61.

In conclusion, the Brillouin scattering study shows a remarkable softening of the LA mode propagating along the ferroelectric c axis in the vicinity of T_C. The sound attenuation shows divergent behavior towards T_C. The temperature intervals of $T^* - T_C$ and $T_B - T_C$ of CBN28 are similar to those of SBN61 under strong random fields. This fact corroborates the same origin of PNRs in CBN28 and SBN61. The broad CP related to the polarization fluctuations along the ferroelectric c axis shows a significant increase in its intensity towards T_C. The relaxation time determined from the CP width shows critical slowing down towards T_C. This fact indicates that CBN28 undergoes but a weakly first-order ferroelectric phase transition with significant pretransitional effects of the order-disorder type and in weak quenched random fields.

[1] L. E. Cross, Ferroelectrics **76**, 241 (1987).
[2] R. Blinc, *Advanced Ferroelectricity*, International Series of Monographs on Physics Vol. 151 (Oxford University Press, Oxford, 2011).
[3] S. Miga, W. Kleemann, J. Dec, and T. Łukasiewicz, Phys. Rev. B **80**, 220103(R) (2009).
[4] W. Kleemann, J. Dec, P. Lehnen, R. Blinc, B. Zalar, and R. Pankrath, Europhys. Lett. **57**, 14 (2002).
[5] J. R. Oliver, R. R. Neurgaonkar, and L. E. Cross, J. Appl. Phys. **64**, 37 (1988).
[6] W. H. Huang, D. Viehland, and R. R. Neurgaonkar, J. Appl. Phys. **76**, 490 (1994).
[7] R. R. Neurgaonkar, W. F. Hall, J. R. Oliver, W. W. Ho, and W. K. Cory, Ferroelectrics **87**, 167 (1988).
[8] A. M. Glass, J. Appl. Phys. **40**, 4699 (1969).
[9] B. Fischer, M. Cronin-Golomb, J. O. White, A. Yariv, and R. R. Neurgaonkar, Appl. Phys. Lett. **40**, 863 (1982).
[10] R. R. Neurgaonkar, W. K. Cory, J. R. Oliver, M. D. Ewbank, and W. F. Hall, Opt. Eng. **26**, 392 (1987).
[11] F. Kahmann, J. Höhne, R. Pankrath, and R. A. Rupp, Phys. Rev. B **50**, 2474 (1994).
[12] M. Wesner, C. Herden, R. Pankrath, D. Kip, and P. Moretti, Phys. Rev. E **64**, 036613 (2001).
[13] S. Podlozhenov, H. A. Graetsch, J. Schneider, M. Ulex, M. Wöhlecke, and K. Betzler, Acta Crystallogr., Sect. B: Struct. Sci. **62**, 960 (2006).
[14] M. A. Kim, P. Wang, J. H. Lee, J. J. Kim, H. Y. Lee, and S.-H. Cho, Jpn. J. Appl. Phys., Part 1 **41**, 7042 (2002).
[15] V. V. Shvartsman, J. Dec, S. Miga, T. Łukasiewicz, and W. Kleemann, Ferroelectrics **376**, 1 (2008).
[16] H. Song, H. Zhang, X. Xu, X. Hu, X. Cheng, J. Wang, and M. Jiang, Mater. Res. Bull. **40**, 643 (2005).
[17] H. Song, H. Zhang, Q. Jiang, X. Xu, C. Lu, X. Hu, J. Wang, and M. Jiang, J. Cryst. Growth **290**, 431 (2006).
[18] M. Eßer, M. Burianek, D. Klimm, and M. Mühlberg, J. Cryst. Growth **240**, 1 (2002).
[19] U. Heine, U. Völker, K. Betzler, M. Burianek, and M. Mühlberg, New J. Phys. **11**, 083021 (2009).
[20] Y. J. Qi, C. J. Lu, J. Zhu, X. B. Chen, H. L. Song, H. J. Zhang, and X. G. Xu, Appl. Phys. Lett. **87**, 082904 (2005).
[21] A. Niemer, R. Pankrath, K. Betzler, M. Burianek, and M. Mühlberg, World J. Condens. Matter Phys. **2**, 80 (2012).
[22] S. D. Prokhorova and S. G. Lushnikov, Ferroelectrics **90**, 187 (1989).
[23] F. M. Jiang and S. Kojima, Phys. Rev. B **62**, 8572 (2000).
[24] S. Kojima, M. Ahart, V. Sivasubramanian, A. A. Bokov, and Z.-G. Ye, J. Adv. Dielectr. **2**, 1241004 (2012).
[25] E. Dul'kin, S. Kojima, and M. Roth, J. Appl. Phys. **110**, 044106 (2011).
[26] E. Dul'kin, J. Petzelt, S. Kamba, E. Majaev, and M. Roth, Appl. Phys. Lett. **97**, 032903 (2010).
[27] R. Pirc and R. Blinc, Phys. Rev. B **76**, 020101(R) (2007).
[28] C. S. Pandey, J. Schreuer, M. Burianek, and M. Mühlberg, Phys. Rev. B **84**, 174102 (2011).
[29] F. Jiang and S. Kojima, Phys. Rev. B **66**, 184301 (2002).
[30] J.-H. Ko and S. Kojima, Appl. Phys. Lett. **91**, 082903 (2007).
[31] S. Tsukada and S. Kojima, Jpn. J. Appl. Phys. **49**, 09ME03 (2010).
[32] T. Łukasiewicz, M. Świrkowicz, J. Dec, W. Hofman, and W. Szyrski, J. Cryst. Growth **310**, 1464 (2008).
[33] S. Kojima, Jpn. J. Appl. Phys. **49**, 07HA01 (2010).
[34] R. Guo, A. S. Bhalla, G. Burns, and F. H. Dacol, Ferroelectrics **93**, 397 (1989).
[35] C. S. Pandey, J. Schreuer, M. Burianek, and M. Mühlberg, Phys. Rev. B **87**, 094101 (2013).
[36] S. Kojima, S. Tsukada, Y. Hidaka, A. A. Bokov, and Z.-G. Ye, J. Appl. Phys. **109**, 084114 (2011).
[37] S. Tsukada, T. H. Kim, and S. Kojima, Appl. Phys. Lett. Mater. **1**, 032114 (2013).
[38] S. Tsukada, Y. Hidaka, S. Kojima, A. A. Bokov, and Z.-G. Ye, Phys. Rev. B **87**, 014101 (2013).
[39] T. Kamiya, K. Nomura, M. Hirano, and H. Hosono, Phys. Status Solidi C **5**, 3098 (2008).